This article is published as part of the *CrystEngComm* themed issue entitled:

Crystal Engineering and Crystallography in the Pharmaceutical Industry

Guest Editors Magali Hickey, Örn Almarsson and Matt Peterson

Published in issue 7, 2012 of *CrystEngComm*

Articles in this issue include:

Highlight
The role of mechanochemistry and supramolecular design in the development of pharmaceutical materials
Amit Delori, Tomislav Friščić and William Jones

Highlight
Pharmaceutical crystallography: is there a devil in the details?
Andrew D. Bond

Paper
The effect of water molecules in stabilizing co-crystals of active pharmaceutical ingredients
Christer B. Aakeröy, Safiyyah Forbes and John Desper

CrystEngComm

Dynamic Article Links

Cite this: *CrystEngComm*, 2012, **14**, 2589

www.rsc.org/crystengcomm

PAPER

Structures and characterization of *m*-nisoldipine polymorphs†

Caiqin Yang,[a] Zhenwei Zhang,[b] Yanli Zeng,[c] Jing Wang,*[a] Yongli Wang[a] and Baoqing Ma*[d]

Received 13th October 2011, Accepted 30th November 2011
DOI: 10.1039/c2ce06359j

m-Nisoldipine, a dihydropyridine calcium ion antagonist, first synthesized in the School of Pharmaceutical Sciences, Hebei Medical University, exhibits two polymorphs A and B with different colors and morphologies. The single-crystal X-ray structure analysis reveals that polymorph A crystallizes in a monoclinic $P2_1/c$ space group with $a = 9.3045(2)$ Å, $b = 16.5991(5)$ Å, $c = 13.0018(3)$ Å, $\beta = 91.539(2)^\circ$ and $Z = 4$, while B crystallizes in a triclinic space group of $P\bar{1}$ with $a = 7.4965(2)$ Å, $b = 11.4692(4)$ Å, $c = 12.3648(5)$ Å, $\alpha = 68.093(2)^\circ$, $\beta = 88.655(2)^\circ$, $\gamma = 81.853(2)^\circ$ and $Z = 2$. The *m*-nisoldipine molecules are connected through N–H···O hydrogen bonds between the carbonyl group and the amine group to form either a wavy chain for A or a linear chain for B. The two polymorphs show distinct physicochemical properties as characterized by IR, Raman, DSC and terahertz pulse spectroscopy. DFT theoretical calculations are also used to simulate the terahertz spectroscopy of the two polymorphs.

Introduction

Polymorphism is the existence of the same chemical compound in more than one crystal structure in the solid-state. In the pharmaceutical industry, the identification of polymorphic forms of drug compounds is of crucial importance. Polymorphs, hydrates and solvates can be produced by a variety of standard pharmaceutical processes.[1–5] Polymorphs of the same drug compound may have very different physical properties that affect bioavailability or processability (*e.g.*, tabletting),[6] and drug regulatory authorities demand detailed information about polymorphism before granting licenses for product distribution.

m-Nisoldipine, 1,4-dihydro-2,6-dimethyl-4-(3-nitrophenyl)-3,5-pyridinedicarboxylic acid methyl 2-methylpropyl ester, is a new dihydropyridine calcium ion antagonist, which was first synthesized in the School of Pharmaceutical Sciences, Hebei Medical University.[7] Compared with its analogues, *m*-nisoldipine significantly increases cardiac output and cardiac index, dramatically reduces the negative inotropic effect on myocardium and has relatively higher selectivity on the thoracic aorta.[8,9] Two polymorphs of *m*-nisoldipine were obtained. It is well known that polymorphism is especially important in connection with shelf life and solubility of pharmaceuticals.[10] For poorly soluble compounds such as *m*-nisoldipine, polymorphism can lead to large variations in bioavailability among different forms.[11] The pharmacokinetics and relative bioavailability of *m*-nisoldipine polymorphs in rats were investigated using a validated LC-MS-MS method.[6] It indicated that polymorphs A and B of *m*-nisoldipine were not bioequivalent. In order to optimize the *m*-nisoldipine drug performance and execute the quality control during manufacture, a series of physicochemical characterizations on the two polymorphs are conducted to gain more understanding of their polymorphic behaviors. Herein we report their IR, Raman, DSC, single-crystal X-ray structures and terahertz spectroscopy coupled with DFT calculations.

Results and discussion

Polymorphs A and B had initially been obtained from different crops of ethanol solvent. Much effort had been made to screen the possible polymorphs from a variety of single solvents or combinations thereof, but only two polymorphs A and B have been obtained so far. Good quality crystals of form A can be obtained from a solution of acetone–EtOH (1 : 1) by a slow evaporation process and polymorph B crystals were obtained from a solution of EtOAc–hexane (1 : 1). The two polymorphs have different colors and morphologies: form A is a yellowish rod and form B is a colorless needle as shown in Fig. 1. As such, polymorph A and B can be visibly identified by their appearances.

Infrared and Raman spectra

The IR and Raman spectra of the two polymorphs display distinct features, which can be employed to distinguish the two

[a]*School of Pharmaceutical Sciences, Hebei Medical University, Shijiazhuang, 050017, China. E-mail: jingwang@home.ipe.ac.cn; Fax: +86311-86266419; Tel: +86311-86265627*
[b]*Department of Physics, Capital Normal University, Beijing, China*
[c]*School of Chemistry and Material Science, Hebei Normal University, Shijiazhuang, China*
[d]*Currently with Sanofi Animal Division, 631 Route 1, North Brunswick, NJ, 08902, USA. E-mail: baoqing.ma@merial.com*

† Electronic supplementary information (ESI) available. CCDC reference number 802078. For ESI and crystallographic data in CIF or other electronic format see DOI: 10.1039/c2ce06359j

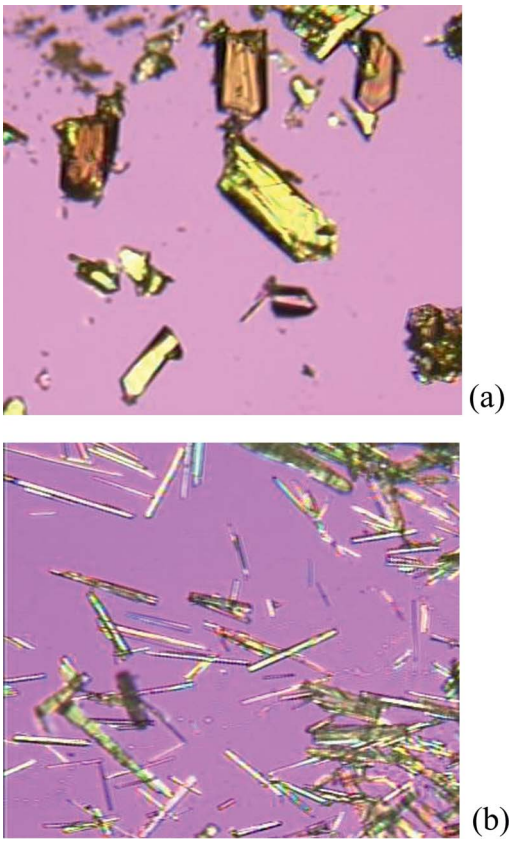

Fig. 1 The morphologies of polymorph A (a) and B (b).

polymorphs for quantitative content analysis. Polymorph A exhibits a single peak at 694 cm^{-1} and a single peak at 1635 cm^{-1} with a shoulder at 1650 cm^{-1}, as opposed to polymorph B which has doublets at 689 cm^{-1} and 704 cm^{-1} and a singlet at 1655 cm^{-1}. Polymorph B has a single peak at 1380 cm^{-1} with a shoulder at 1394 cm^{-1}, whereas polymorph A shows a single peak at 1399 cm^{-1} with a shoulder at 1380 cm^{-1}. Additional strong peaks for polymorph B occur at 2835, 1326, 1305, 1147, 1254 and 1699 cm^{-1}. Peaks at 586 cm^{-1} and 636 cm^{-1} for polymorph B are stronger than those of polymorph A.

The Raman spectrum for polymorph A exhibits a significant profile difference from that of polymorph B. The feature peaks at 586 cm^{-1}, 1669 cm^{-1} and 1698 cm^{-1} for form A contrast with those at 1222 cm^{-1} and 1677 cm^{-1} for form B. The striking Raman peak features for form A and B provide a practical application in polymorph identification, drug content uniformity and PAT as the Raman technique coupled with microscopic images gains broad and intensive use in modern pharmaceutical industries.

DSC analysis

Differential scanning calorimetry (DSC) showed a melting point of 135.8 °C and 129.2 °C for polymorphs A and B with the corresponding enthalpy of 82.3 J g^{-1} and 88.3 J g^{-1}, respectively. No thermal-induced polymorphic transformation is observed during the course of heating. According to the polymorph rule of heat of fusion,[12,13] which states that if the higher melting polymorph has the lower heat of fusion, then the two polymorphs are enantiotropic, forms A and B are enantiotropically related. The conversion temperature in solution is about 47 °C as obtained from van't Hoff plot.[14] Form A is the thermodynamically stable one below the conversion temperature. The pharmacokinetic studies of oral dosage of polymorphs A and B administrated to rats show that form B has relatively higher bioavailability compared with form A.[6] It is consistent with thermodynamic stability of form A, which has low solubility and dissolution rate. It also indicates the importance of polymorph screening and form selection in drug formulation.

Single-crystal X-ray diffraction

The single-crystal X-ray diffraction analyses reveal that the two polymorphs crystallize in different crystal systems. Form A belongs to a monoclinic $P2_1/c$, while form B crystallizes in a triclinic $P\bar{1}$. Their molecular structures are illustrated in Fig. 2. They exhibit a different molecular conformation as presented by their superimposed structures in Fig. 3. The two carbonyl groups from the isobutyl ester and methyl ester point in the same direction in form B, while they are opposed in form A due to the rotation of the single C–C bond. The nitrobenzene plane in both forms is almost perpendicular to the diene plane with slightly different intersecting angles of 84.23° and 89.55° for A and B, respectively. In both polymorphs, the *m*-nisoldipine molecules are linked through the N–H···O hydrogen bonds [N2···O3a = 2.927(2) Å and 3.089 Å, N2–H2A···O3a = 139.1° and 171.0° for A and B, respectively; a = x, $-y$ + 1/2, z + 1/2 for A and x + 1,

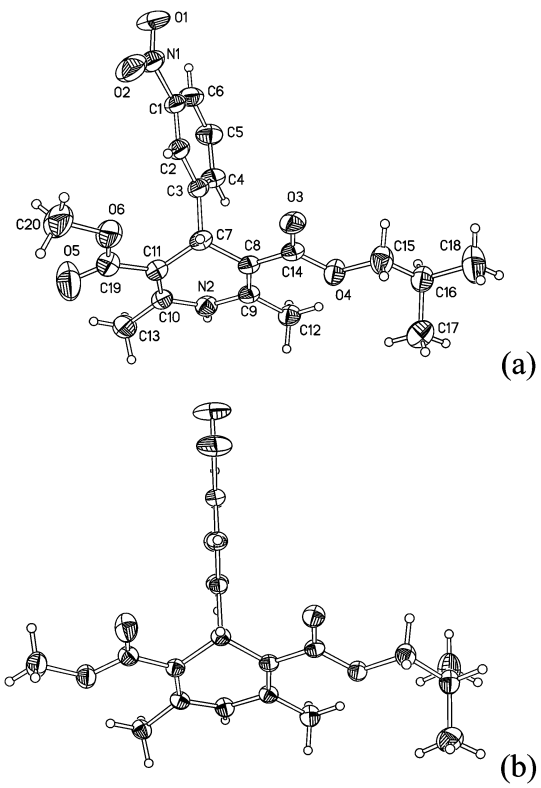

Fig. 2 The molecular structure of *m*-nisoldipine polymorph A (a) and B (b) with 35% ellipsoid probability.

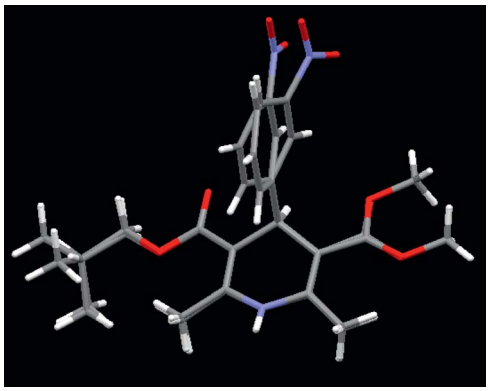

Fig. 3 An overlapping of *m*-nisoldipine in polymorph A and B.

y, *z* for B], resulting in a 1D hydrogen-bonded structure (Fig. 4). Although the connections between *m*-nisoldipine molecules are same, the two 1D structures are quite different. In A, the hydrogen bonding angle is bent and the adjacent *m*-nisoldipine molecules are twisted, leading to a wavy chain. The dangling isobutyl groups from adjacent wavy chains are intercalated together by van der Waals interactions, giving rise to an undulating layer. These layers are further stacked to produce a 3D packing (Fig. 5a). However, in B, the hydrogen bond orientation is close to linear and the adjacent *m*-nisoldipine molecules form a linear ribbon motif. The nitrobenzene moieties from the neighboring ribbon are held together by π–π stacking with the centroid distance being 4.056 Å (shown in Fig. 6) to form a ladder-like motif. These ladders are packed together by van der Waals interactions to generate a 3D network (Fig. 5b).

The calculated density of form B is 1.322 g cm^{-3}, which is significantly larger than that of A (1.285 g cm^{-3}). This could be related to the presence of strong aromatic π–π stacking in form B, which gives the closest packing. Obviously, the density rule is not applicable herein due to the presence of hydrogen bonding interactions in the structure.[12]

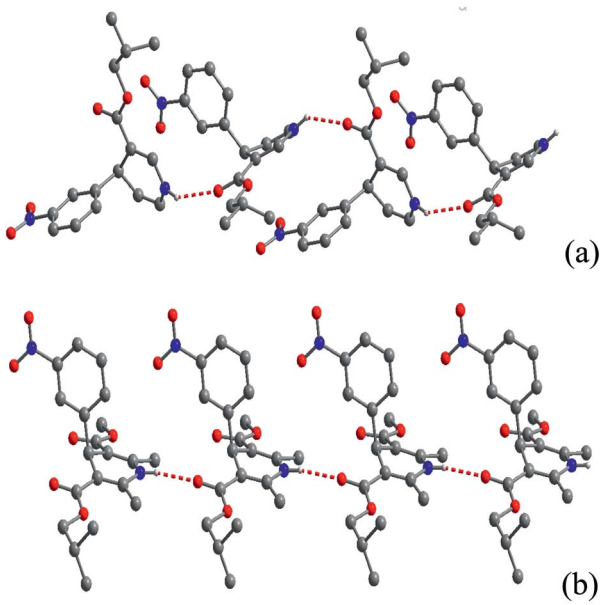

Fig. 4 The 1D chain constructed by N–H···O hydrogen bonding between *m*-nisoldipine in polymorph A (a) and B (b).

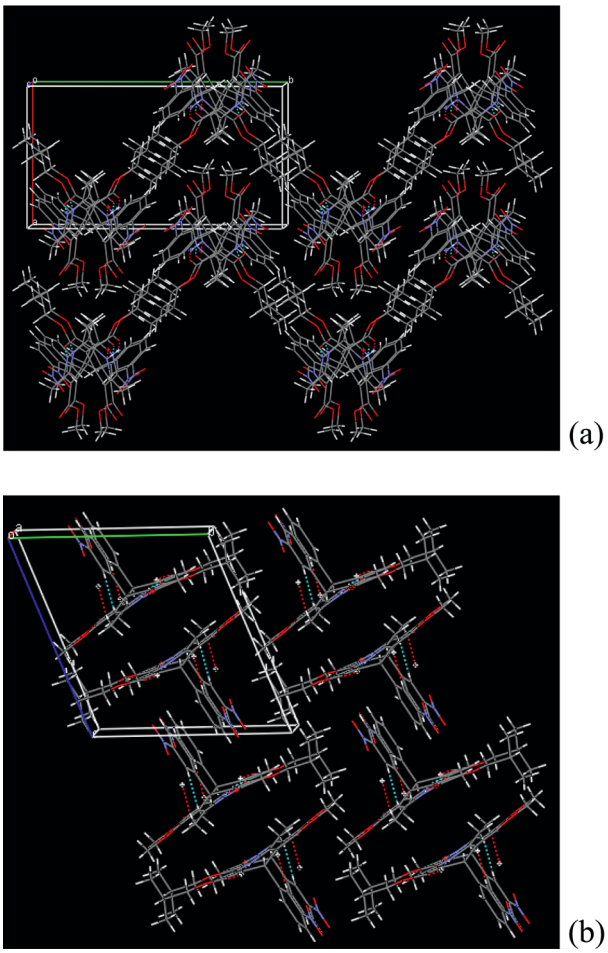

Fig. 5 The overall packing diagram of *m*-nisoldipine in the unit cell for polymorph A (a) and B (b).

TPS characterization and DFT theoretical calculations

Terahertz spectroscopy was carried out for polymorphs A and B as this technique is very sensitive to the intermolecular interactions. An overlay of the terahertz spectra for polymorphs A and B is shown in Fig. 7. The spectrum of form A exhibits major peaks at 0.23, 0.75, 1.81 THz, and smaller peaks at 0.6 and 1.1 THz, while the form B spectrum has prominent peaks at 0.50, 0.70, 0.88, 1.23 and 1.43 THz with low intensity peaks at 1.60 and 1.77 THz. In order to understand and interpret these terahertz absorption spectra, DFT calculations were performed to simulate the structural interaction and the corresponding absorption, which is used to assign the determined terahertz absorption to vibrational spectra. In polymorph A, the low frequency features at 0.23 and 0.4 THz are attributed a symmetric bending of the N–H···O hydrogen bond at 0.25 and 0.34 THz. The latter results from the vibrations of whole molecule frameworks in the dimer (Fig. 8a). The strong peak at 0.75 THz is assigned to an asymmetric bending mode of the N–H···O hydrogen bond at 0.73 THz (Fig. 8b). The absorption at 1.81 THz could come from the vibration of the single molecule framework in the dimer (Fig. 8c:A, 1.81 THz).

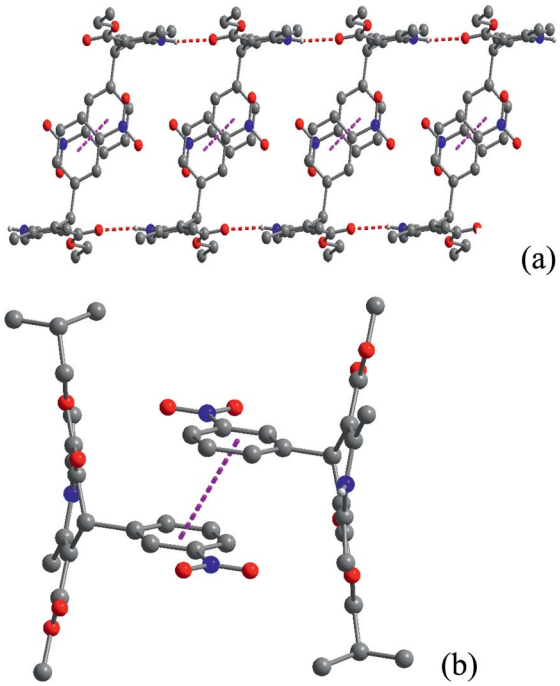

Fig. 6 The 1D ladder-like structure connected by both hydrogen bonding and the π–π stacking between the phenyl ring in polymorph B (a) together with the side view (b).

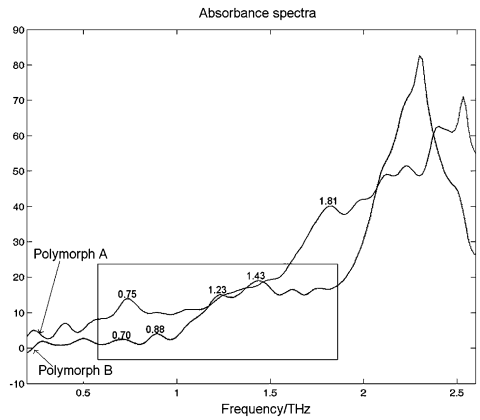

Fig. 7 Absorbance spectra of *m*-nisoldipine polymorph A and B The insert highlights the region from 0.7 to 1.8 THz where there are considerable changes in the terahertz spectrum between the two polymorphs.

In form B, there are four peaks at 0.30, 0.51, 0.70 and 0.88 THz from 0.2 to 0.9 THz. The corresponding calculation has four modes at 0.25, 0.51, 0.69 and 0.93 THz. It was noted that the THz spectrum in form B has an equal spaced absorption at an approximate interval of 0.2 THz in this range. The calculation indicates that these modes are predominantly involved with the motions of π–π stacking between the phenyl rings in the dimers related by an inversion center (Fig. 9). The peaks at 1.23 and 1.43 THz are assigned to the calculated asymmetric bending mode of the N–H···O hydrogen bond at 1.09 and 1.45 THz (Fig. 10a,b). The strong peak at 2.32 THz is associated to the calculated stretch vibration of the N–H···O hydrogen bond (Fig. 10c).

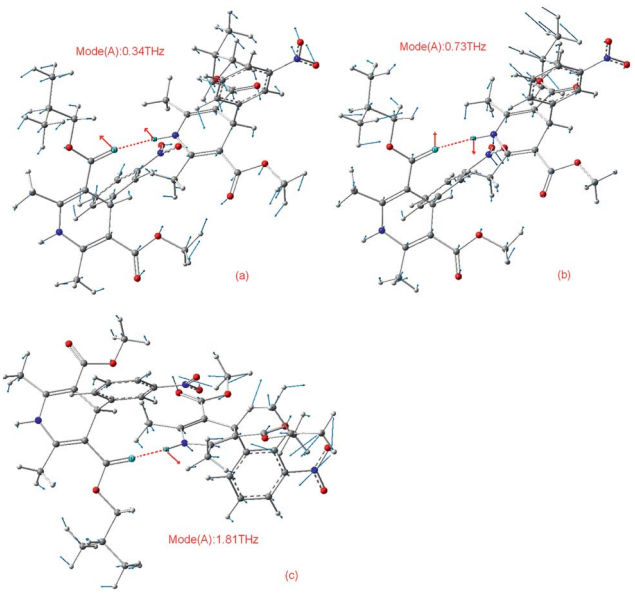

Fig. 8 Modes of vibration of the N–H···O hydrogen bond in polymorph A.

The structural and spectral DFT simulation were able to assign most of the experimental spectral features to one or more of the calculated vibrational modes. It provides us with a good insight into the molecular interactions in polymorphs A and B. The markedly different terahertz features of form A and B suggest that the terahertz spectrum is a useful tool to identify polymorphs A and B.

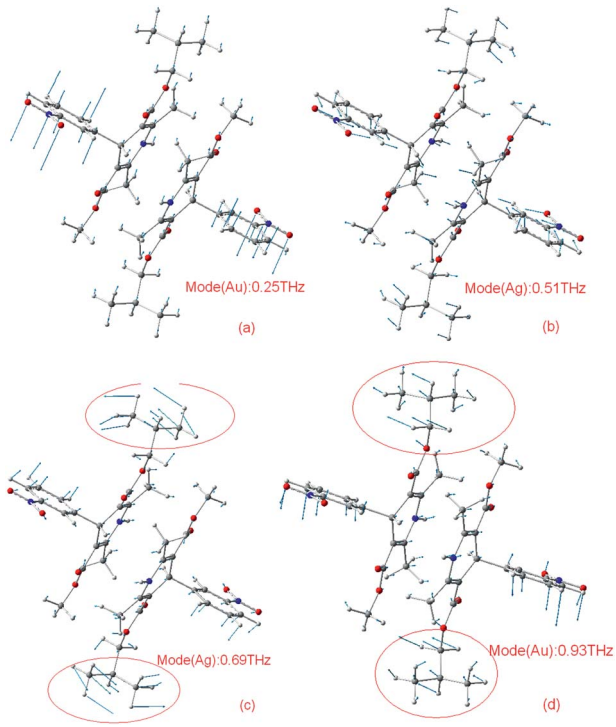

Fig. 9 Modes of vibration of π–π stacking between the phenyl rings in polymorph B.

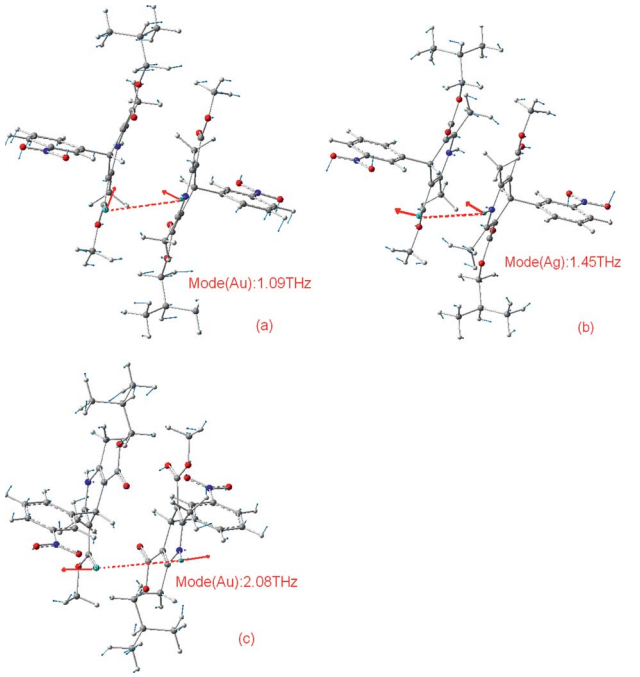

Fig. 10 Modes of vibration of the N–H···O hydrogen bond in polymorph B.

Conclusions

Two polymorphs of *m*-nisoldipine were discovered and physically characterized by a series of solid-state techniques. They can be discriminated by their visible appearance as they have different colors and morphologies. The single-crystal structure shows that the two polymorphs are classified as conformational polymorphs, with different packing motifs. Forms A and B have an enantiotropic relationship with a conversion temperature of 47 °C and form A is the thermodynamically stable form below this temperature. The IR, Raman and terahertz spectra show distinctive peaks, which can be used to distinguish polymorphs A and B. The terahertz absorption was further interpreted based on the DFT calculations and more insight into the intermolecular interaction was gained.

Experimental section

Preparation

The compound 1,4-dihydro-2,6-dimethyl-4-(3-nitrophenyl)-3,5-pyridinedicarboxylic acid methyl 2-methylpropyl ester was synthesized according to the procedure given in the Chinese patent.[7] Efforts were made to crystallize the compound in different solvent systems, such as EtOH, acetone, EtOAc–hexane and acetone–EtOH to evaluate the influence of change in polarity of the solvents. Single crystals of polymorph A were grown from a solution of acetone–EtOH (1 : 1) by a slow evaporation process and those of the polymorph B were obtained from a solution of EtOAc–hexane (1 : 1).

Characterization

DSC studies were performed on a Perkin-Elmer Pyris1 apparatus employing a heating rate of 5 °C min^{-1} and N_2 gas as the purging gas at a flow rate of 20 mL min^{-1}. Infrared spectra were recorded from 4000–400 cm^{-1} for form A and B using a EQUINOX 55 (Bruker) FT-IR spectrometer. Each spectrum was the average of 200 scans using a spectral resolution of 4 cm^{-1}. Raman spectra were recorded in the 500–2000 cm^{-1} range by measuring in backscattering geometry and using a Bruker spectrometer using a 647.1 nm mixed argon–krypton laser (50 mW). All terahertz measurements were made using a TPI™ spectra 1000 transmission spectrometer (TeraView Limited, Cambridge, UK). Samples were measured at an instrument resolution of 2–3 cm^{-1} over the range of 0–3 THz. Data was acquired and processed using OPUS™ (Bruker Optics, Germany) software.

DFT calculations

Calculations were performed on polymorphs A and B, taking molecular structures from the X-ray determined coordinates as the starting geometries. Then, equilibrium geometries were fully optimized at the DFT B3LYP/6-31G** level using the GAUSSIAN-03 program package.[15] Harmonic frequencies were calculated based on the equilibrium geometries.

Crystallography

Crystal data: Form A, $C_{20}H_{24}N_2O_6$, M_r 388.41, Monoclinic, $P2_1/c$, T = 298(2) K, a = 9.3045(2) Å, b = 16.5991(5) Å, c = 13.0018(3) Å, β = 91.539(2)°, Z = 4, V = 2007.36(9) Å^3, ρ_{calc} = 1.285 Mg m^{-3}, R_1 [$I > 2\sigma(I)$] = 0.0688. Form B, $C_{20}H_{24}N_2O_6$, M_r 388.41, Triclinic, $P\bar{1}$, T = 298(2) K, a = 7.4965(2) Å, b = 11.4692 (4) Å, c = 12.3648(5) Å, α = 68.093(2)°, β = 88.655(2)°, γ = 81.853(2)°, Z = 2, V = 975.89(6) Å^3, ρ_{calc} = 1.322 Mg m^{-3}, R_1 [$I > 2\sigma(I)$] = 0.0676. X-ray reflections were collected on Bruker SMART-APEX CCD diffractometer (Mo-Kα radiation, λ = 0.71073 Å) with a 10 s exposure time. Empirical absorption corrections were applied using the multi-scan method. The structures were solved by the direct method and refined by full-matrix least-squares on F^2 using the SHELX program with anisotropic thermal parameters for all non-hydrogen atoms. Hydrogen atoms were placed on calculation positions.

Acknowledgements

The financial support for this work by the Hebei Province Natural Science Fund of China (2008001072), Science Fund (2009148) of the Education Department and Science Fund (20090059) of the Health Department of Hebei Province of China are greatly acknowledged. This work was also funded by the National Keystone Basic Research Program (973 Program) under Grant No. 2007CB310408.

References

1 R. S. Agam, B. Simon and X. Francis, *Cryst. Growth Des.*, 2004, **4**, 1091.
2 R. Barbas, F. Mart, R. Prohens and C. Puigjaner, *Cryst. Growth Des.*, 2006, **6**, 1463.
3 Z. B. Ma and B. Moulton, *Cryst. Growth Des.*, 2007, **7**, 196.
4 W. W. Porter, III., S. C. Elie and A. J. Matzger, *Cryst. Growth Des.*, 2008, **8**, 14.
5 B. Y. Lou, D. Bostrom and P. V. Sitaram, *Cryst. Growth Des.*, 2009, **9**, 1254.

6 H. R. Wang, L. T. Zhang, Q. Wang, Z. F. Yuan and M. Li, *J. Chromatogr., B: Anal. Technol. Biomed. Life Sci.*, 2006, **835**, 71.
7 F. Yuan, Y. Wu, H. Nie, Y. Yan, C. Bao, Z. Chen, Y. Du, J. Zhao, D. Man and H. Geng, CN93103759.X. Briefly, isobutyl acetoacetate (4.2 g) and 3-nitrobenzaldehyde (3.8 g) were dissolved in toluene (20 mL) in a reactor. The solvent was removed under reduced pressure after the solution was left standing for 12 h. Then methyl acetoacetate (2.9 g) and 95% ethanol (15 mL) were added into the above reactor. The mixture was refluxed in the presence of 25% ammonia for 8 h. The solvent was removed under reduced pressure, and the residue was dissolved in 95% ethanol (18 mL) and left standing for 12 h. The final product was obtained by filtration and re-crystallization in ethanol. Polymorphs A and B appeared in the upper and lower part of the ethanol solvent, respectively, during cooling of the hot ethanol solvent in the refrigerator.
8 Y. Gao, Y. Li and S. Fu, *China Pharmacol. Bull.*, 1990, **6**, 114.
9 Y. Gao, Y. Li and S. Fu, *J. China Pharmacol. Toxicol.*, 1990, **4**, 21.
10 S. Byrn, R. Pfeiffer, M. Ganey, C. Hoiberg and G. Poochikian, *Pharm. Res.*, 1995, **12**, 945.
11 S. R. Chemburkar, J. Bauer, K. Deming, H. Spiwek, K. Patel, J. Morris, R. Henry, S. Spanton, W. Dziki, W. Porter, J. Quick, P. Bauer, J. Donaubauer, B. A. Narayanan, M. Soldani, D. Riley and K. McFarland, *Org. Process Res. Dev.*, 2000, **4**, 413.
12 J. Bernstein, *Polymorphism in Molecular Crystals*, Oxford University Press, 2002.
13 H. G. Brittain, *Polymorphism in Pharmaceutical Solids*, Informa Healthcare, 1999.
14 C. Yang, J. Wang, Y. Wang, Y. Lin and X. Tao, *unpublished results*.
15 M. J. Frisch, G. W. Trucks, H. B. Schlegel, G. E. Scuseria, M. A. Robb, J. R. Cheeseman, J. A. Montgomery, Jr., T. Vreven, K. N. Kudin, J. C. Burant, J. M. Millam, S. S. Iyengar, J. Tomasi, V. Barone, B. Mennucci, M. Cossi, G. Scalmani, N. Rega, G. A. Petersson, H. Nakatsuji, M. Hada, M. Ehara, K. Toyota, R. Fukuda, J. Hasegawa, M. Ishida, T. Nakajima, Y. Honda, O. Kitao, H. Nakai, M. Klene, X. Li, J. E. Knox, H. P. Hratchian, J. B. Cross, V. Bakken, C. Adamo, J. Jaramillo, R. Gomperts, R. E. Stratmann, O. Yazyev, A. J. Austin, R. Cammi, C. Pomelli, J. Ochterski, P. Y. Ayala, K. Morokuma, G. A. Voth, P. Salvador, J. J. Dannenberg, V. G. Zakrzewski, S. Dapprich, A. D. Daniels, M. C. Strain, O. Farkas, D. K. Malick, A. D. Rabuck, K. Raghavachari, J. B. Foresman, J. V. Ortiz, Q. Cui, A. G. Baboul, S. Clifford, J. Cioslowski, B. B. Stefanov, G. Liu, A. Liashenko, P. Piskorz, I. Komaromi, R. L. Martin, D. J. Fox, T. Keith, M. A. Al-Laham, C. Y. Peng, A. Nanayakkara, M. Challacombe, P. M. W. Gill, B. G. Johnson, W. Chen, M. W. Wong, C. Gonzalez and J. A. Pople, *GAUSSIAN 03 (Revision D.01)*, Gaussian, Inc., Wallingford, CT, 2004.

